

Phase Current Reconstruction based on Rogowski Coils Integrated on Gate Driver of SiC MOSFET Half-Bridge Module for Continuous and Discontinuous PWM Inverter Applications

Slavko Mocevic, Jun Wang,
Rolando Burgos, Dushan Boroyevich
Center for Power Electronics Systems
Virginia Polytechnic Institute and State University
Blacksburg, VA 24061, USA
slavko7@vt.edu

Marko Jaksic, Mehrdad Teimor,
Brian Peaslee
General Motors
Global Propulsion Systems
Pontiac, MI 48340, USA
marko.jaksic@gm.com

Abstract—This paper seeks to explore the benefits brought by PCB-embedded Rogowski switch-current sensors integrated on the gate driver of a 1.2 kV, 300 A SiC MOSFET half-bridge module. They collect two MOSFET switch currents in a manner of high magnitude, high bandwidth, and solid signal isolation. Apart from high bandwidth switch-current signals being used for short-circuit detection, they are further utilized for phase current reconstruction. The fundamentals of the phase current reconstruction done by subtraction of switch currents are presented in the paper as well as phase current sensor performance during continuous and discontinuous PWM schemes for three-phase inverter applications. Presented principles can be applied to any half-bridge power module. A three-phase inverter prototype has been built and operated in both continuous and discontinuous PWM mode. On this setup, the performance and limitations of phase-current reconstruction are experimentally validated for both PWM schemes.

Index Terms—Current sensor, continuous PWM, discontinuous PWM (DPWM), gate driver, Rogowski switch-current sensor, magnetic influence, phase current reconstruction, SiC MOSFET

I. INTRODUCTION

Silicon carbide (SiC) MOSFETs semiconductor power devices are becoming more available due to continuing trend of decrease in price, increased usage in industry applications and their growing mass production. They are slowly becoming global solution in applications such as power inverters substituting conventional Si solutions such as IGBTs and MOSFETs due to their fast switching speed, low on-state resistance, high breakdown electric field and high working temperature [1], and [2].

Even though SiC MOSFET devices have showed superior performance, reliability during failure modes, such as short-circuit (SC), may put an additional concern on utilization of these devices due to a reported very narrow SC withstand

window which puts additional challenge to response time critical of protection. According to [3, 4] desaturation (DeSat) protection (most exploited in IGBT applications) necessary blanking time and sensitivity to temperature, might render it unsuitable for SiC device protection. Due to a high-density, high-efficiency trends and a necessity of introducing a new fast and reliable SC protection method for SiC MOSFET devices, PCB-embedded Rogowski switch current sensor (RSCS) integrated on the GD has been developed [5, 6] for the 1.7 kV SiC MOSFET half-bridge module. It has high sensing range, high bandwidth, low response delay, high noise immunity, high accuracy, and high density, making it capable of detecting shoot-through SC events withing 80 ns, protecting the device under 1.2 μ s with implemented soft turn-off technique.

To increase power density and to reduce overall system cost and weight, other sensors, such as a current sensor as a crucial part of the closed-loop system, could be possibly appropriated for SiC inverter applications. In inverter applications, widely used phase current transducers are Hall-effect sensors, current shunts, current transformers and Rogowski coils due to benefits that they exhibit over other sensing methods. Hall-effect sensors (DC and AC measurements) are basically standard for phase current measurement due to its simplicity, accuracy, reliability, hassle-free maintenance and fully isolated structure. However, due to higher density trends in power electronics, these transducers are considered bulky, expensive, susceptible to external magnetic fields and have complicated construction, especially in the closed-loop format [7]–[10]. The simplest and most cost-effective alternative is the use of current shunts, which can be located in series with bottom power devices or in DC bus using single shunt. The biggest drawback of using shunts are that they are intrusive to the circuit introducing additional losses to the system, thus contradicting high efficiency trends [7, 11, 12]. Furthermore, for realizing next generation circuits using SiC MOSFETs, use of first shunt method may be unacceptable due to addition

Work supported by General Motors and by the U.S. Department of Energy, Vehicle Technologies Office (VTO), under Award Number DE-EE0007285.

of parasitic inductance in the system, thus degrading switching performance. Current transformers (CT) have been widely used for AC current sensing with very high bandwidth, providing galvanic isolation, consuming little power, and having low losses. Even with being non-intrusive, due to its bulkiness, lower accuracy, and inability to measure DC currents, this type of measurement is not popular in inverter applications [7]. The Rogowski coil is compact, simple structure, non-intrusive method able of measuring high frequency, high magnitude AC currents without saturation (air core), exhibiting good linearity due to absence of magnetic material. However, it is not extensively used in inverters since it is unable to measure DC currents and is inaccurate at low frequencies ($<20\text{Hz}$), due to its principle of operation based on detection of flux change [7], and [9].

As mentioned, high bandwidth device current measurement with RSCSs is already been utilized for the protection purposes. Further utilization of switch currents will enable reconstruction of the phase current on the GD itself via simple manipulation, which is described in Section II. This can possibly allow increase in power density and efficiency since existing mentioned current sensing methods (bulky Hall-sensor, lossy current shunts etc.) can be eliminated. Phase current information for continuously switched pulse-width modulation (PWM) inverters can then be sent back to the main controller for control purposes, without any additional effort from it in reconstruction, or any additional current sensing in the system, which is described in Section III. For discontinuous PWM schemes, due to drifting of the current sensor during clamped periods, current information sent back for controller will not be accurate. However, simple manipulation of main controller will be required in order to obtain valid phase current measurement, which is described in Section IV. Influence of the adjacent magnetic fields on Rogowski coils is described in Section V. Focus of this paper will not be towards developed GD, RCSC and short-circuit performance but towards evaluation of phase current sensor employed in inverter application.

II. PHASE CURRENT RECONSTRUCTION PRINCIPLE ON GATE DRIVER

A. Principle of Operation

Fig.1 shows one inverter phase leg together with indicated typical waveforms. From t_0 to t_1 , while the S2 is on, the RSCS that is sensing the bottom switch current provides the voltage proportional to the current. During this first part of the PWM sequence, S1 is off, meaning that the output voltage of the top RSCS is equal to zero. In the rest of the switching cycle period (t_1 to t_2) when the S1 is on, the situation is reversed. The top RSCS provides voltage proportional to the current through the switch, while the voltage of the bottom RSCS is clamped to zero since no current is flowing through the S2. By knowing each switches current in the complete switching cycle, outputting the phase current from the GD is possible by constantly subtracting these two switch currents.

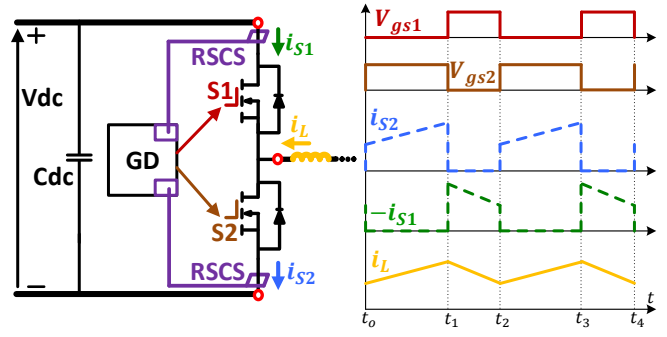


Fig. 1. Phase current reconstruction principle

To obtain phase current information, measurements from RSCS-s need to be subtracted on the common ground of the GD, which in this case is on the same ground as controller. According to this and the fact that introducing new isolation barrier with associated coupling capacitance if Rogowski coils were to be placed on the isolated ground, coils were placed on the primary GD ground. This makes current measurement system fully isolated. Analog information of reconstructed current will be considered in order to emulate commercial current measurement and compare results with it. However, digital reconstruction of the phase current, instead of analog reconstruction with OpAmp and resistor network, is selected and detailed diagram is shown on the Fig.2. Reasons for digital reconstruction are further discussed in the [13].

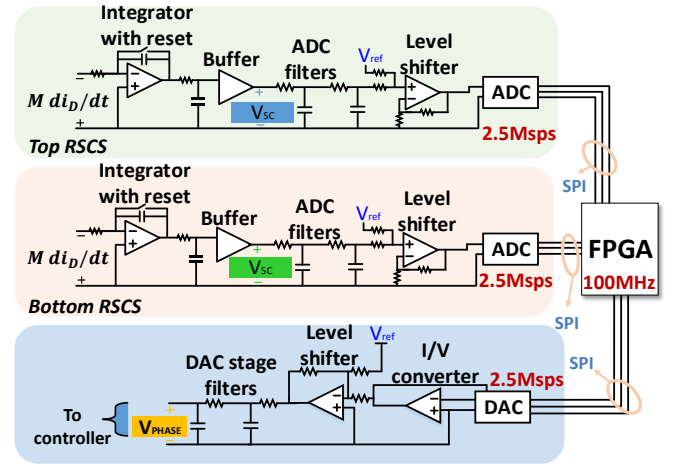


Fig. 2. Detailed diagram of digital phase current reconstruction

From Fig.2 it can be seen that the switch current sensor is composed by a Rogowski coil and a signal processing circuit which mostly comprises of integrator circuit and reset. di_D/dt information, scaled with a factor of mutual inductance, is approximate voltage induced at the output of the Rogowski coil (1).

$$V_{coil} = M \frac{di_D}{dt} \quad (1)$$

The integrator is employed with the coil to convert the

di_D/dt information back to the current information (2). Active integrator is employed instead of passive RC integrator, to reduce the low frequency bandwidth, extending the coil bandwidth [14].

$$V_{int} = \frac{1}{RC} \int V_{coil} dt + C_{int} = \frac{M}{RC} i_D + C_{int} \quad (2)$$

Since an ideal integrator does not exist, integration error will accumulate over time. It must be eliminated in order to sense correct values of the switch current. To resolve the problem, an active reset switch is added to the integrator to reset the output to zero when the SiC MOSFET is switched off, thus avoiding drifting of the sensor. Eventually the switch current sensor can sense pulsating current with correct amplitude and high accuracy. The output voltage of the integrator is filtered with the 30 MHz high frequency RC filter, resulting in a high bandwidth sensed current that can be used for both protection and phase current reconstruction. After buffer stage, information that is being used for phase current reconstruction is filtered with a cutoff frequency of 3.3 MHz, to eliminate high frequency ringing during switching instances. The OpAmp level shifter is employed to adjust the signal to the proper values for ADC sampling. A high precision 14-bit ADC with sample rate of 2.5 Msps is chosen in order to reduce delay of the current measurement. Two ADCs for top and bottom switch currents are synchronized, and they work in non-stop sampling mode in order to send sampled data in the FPGA at the same time instances. When FPGA receives information, it performs digital subtraction of data in one clock cycle (10 ns). After subtraction, FPGA starts placing that information on the DAC SPI bus. A 16-bit, 2.5 Msps, 50 MHz SPI clock rate DAC with small settling time is chosen to convert information back to analog without creating a lot of additional delay. Since the DAC is a single-channel current output, an additional external I/V converter OpAmp is employed. After the I/V OpAmp there is additional level shifter to invert and adjust current information. Another two-stage RC filter with cutoff frequency of 3.3 MHz is employed to filter out the staircase waveform coming from the DAC reconstruction process. Based on the previous analysis, the phase current delay can be expected to be in the range of 1.6 μ s which is shown in the (3):

$$\begin{aligned} t_{dly}^{PhsC} &= t_{dly}^{intg} + t_{dly}^{RC} + t_{dly}^{2stageRC} + t_{dly}^{lvlshft} + t_{dly}^{ADC} + \\ &\quad t_{dly}^{FPGA} + t_{dly}^{DAC} + t_{dly}^{lvlshft} + t_{dly}^{2stageRC} \\ &= 40ns + 30ns + 300ns + 40ns + 400ns \\ &\quad + 10ns + 400ns + 40ns + 300ns = 1.56\mu s \end{aligned} \quad (3)$$

Phase current delay of around 1.6 μ s is not severe for inverter stage electric vehicle applications with intended switching frequency of 30 kHz and can be compensated on main controller level.

B. Gate Driver Prototype and Inverter

The functional circuit design of gate driver is carried out based on that described in prior research [3], and [5]. As

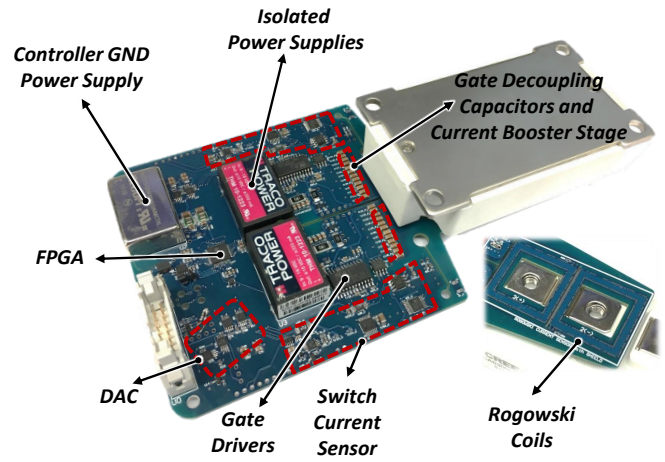


Fig. 3. 1.2 kV gate driver prototype with PCB-embedded Rogowski coils

far as the PCB-embedded RSCS is concerned, since a 1.2 kV, 300 A Cree module has the same package as the 1.7 kV 300 A version, the same principal and design procedure is followed as in other work reported in [6]. Fig.3 shows the prototype GD board with RSCS and a phase current sensor. The experimental inverter test setup is shown in Fig.4. Developed GDs with phase current sensors are connected to the 1.2 kV, 300 A SiC MOSFET module. The inverter is mounted on the water-cooled cold-plate to avoid overheating during continuous testing. Used source was able to provide 100 kW max, 1 kV max, 100 A max. Inverter DC voltage was set to be 600 V. The load is consisted of a 0.27 mH three phase inductor together with a 1.7 resistor in each phase. Voltage and current probes such as Rogowski coils and Hall effect sensor, against which developed sensor was compared, are also shown on the Fig.4.

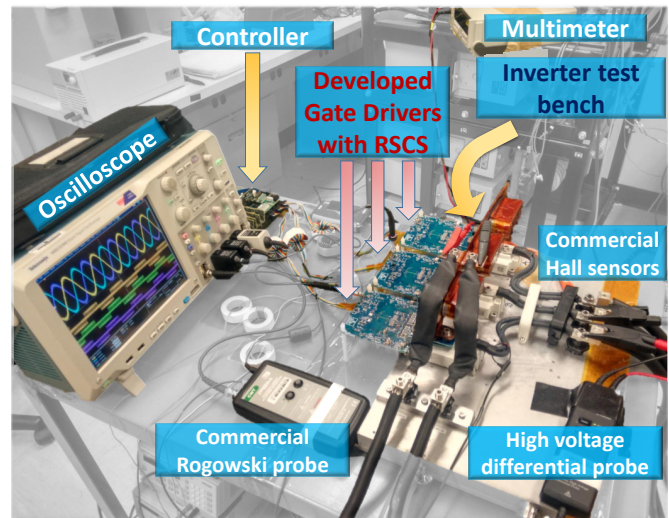


Fig. 4. Three phase inverter experimental setup

III. PHASE CURRENT SENSOR BEHAVIOUR IN CONTINUOUS PWM SCHEMES

Modulation used to control inverter is open loop sinusoidal PWM (SPWM), due to implementation simplicity and the fact that for sensor validation and evaluation, PWM scheme is not essential. Modulation index is set to be 0.9. Since turn-on and turn-off time of the switches is very fast $< 100 \text{ ns}$ (very low gate source external resistance $R_{GS}^{on} = 0.1 \Omega$, $R_{GS}^{off} = 0.05 \Omega$ were used in order to push the transient speed and reduce switching losses), dead-time in this case is set to be 300 ns . The switching frequency was 30 kHz , while modulation (line) frequency was 400 Hz .

Fig.5 shows the reconstructed current from one of the phases, together with the switches currents in the corresponding phase, alongside with the corresponding line-to-line voltage (purple). It is easily observable that the on board reconstructed phase current waveform (blue) is the result of subtracting top switch current (red) from the bottom switch current (green).

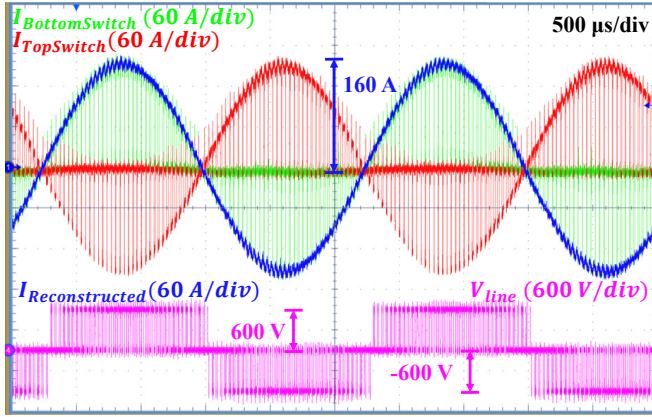


Fig. 5. Reconstructed phase current of the inverter phase

Fig.6 shows comparison between Rogowski coil reconstructed phase current measurement (blue) with the commercial Hall effect sensor measurement from LEM (pink). The delay is consistent and its value is $1.6 \mu\text{s}$ as previously discussed. The reconstructed phase current follows the commercial measurement very well in both amplitude and phase. Furthermore, cyan color waveform represents error between these 2 measurements. Error waveform consists of 2 parts. First part is contributed by the $1.6 \mu\text{s}$ delay, which can be labeled as a phase delay. As discussed, this delay can be overcome on the controller level, delaying the sampling by the same amount of time during one PWM cycle. Second part is contributed by the actual sensor inaccuracy compared to commercial measurement. According to the [13], relative reconstruction error ranges from 0.5–3 % in a high current case where for low currents reconstruction error is slightly higher reaching up to 8 % for switching frequencies between 10 kHz and 100 kHz . However, for any case absolute values error is always smaller than 3 A making it suitable for control.

Linearity error was maximum 2.5 % for whole temperature range.

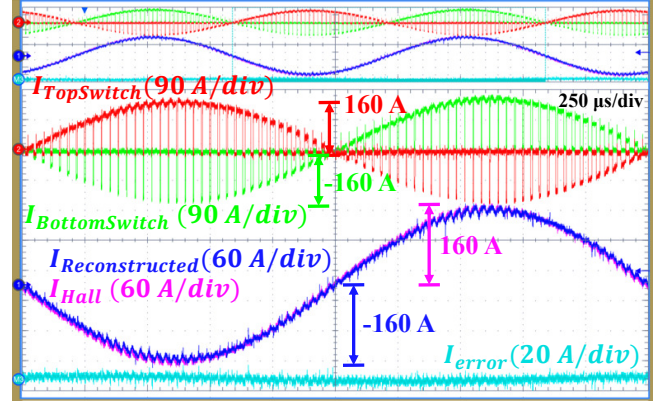


Fig. 6. Comparison with the commercial phase current measurement

Fig.7 presents a normalized spectral comparison of on board phase current sensor with 2 commercial phase current sensors, Rogowski (from PEM) and Hall-effect sensor (from LEM). Reconstructed phase current sensor contains more noise in high frequency region than both of commercial measurement which is expected. On board phase current sensor is located on GD board on the path of the common mode current coming from the device switching. Even though different mitigation techniques were employed to minimize that noise, not all of it could be suppressed. This noisier part is observable on the multiple of switching instances (30 kHz , 60 kHz etc.) where blue (on board sensor) results in higher peaks than commercial measurements. One more important part that can be also noticed from frequency spectrum is that between 400 Hz and 30 kHz there is no significant harmonics in the spectra, which is expected and experimentally verified. Most of spectral energy is located on the 400 Hz as expected, since that is the modulation frequency used, and it overlaps with commercial measurements.

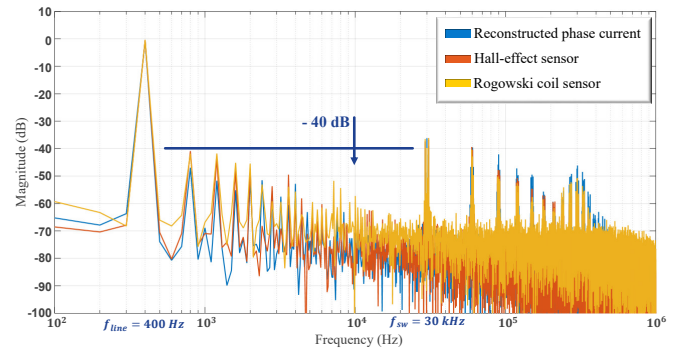


Fig. 7. Frequency spectra of the 3 different phase current measurement techniques

IV. PHASE CURRENT SENSOR BEHAVIOUR IN DISCONTINUOUS PWM SCHEMES

A. Sensor Problem during Discontinuous PWM

As seen from Section III and [13], in continuous PWM systems switch current sensors will work almost perfectly for switching frequencies above 10 kHz, which are in the SiC MOSFET domain. However, when there is a PWM signal longer than 100 μs , developed sensor starts being inaccurate and invalidates the sensor output since integration error becomes severe. This means that during discontinuous PWM (DPWM), during clamped periods longer than 100 μs where there is no reset signal, the measurement of the switch sensor will be invalid due to accumulated integration error. This eventually makes the phase current sensor measurement (created by subtraction of two switch currents) wrong during these clamped periods when switches of the corresponding phase are not switching. Closed loop current control cannot be realized based on this current measurement since periods of severe inaccuracy in phase current exist. Fig.8 shows one example of RSCS and phase current sensor behavior during DPWM in inverter application. It can be seen that as long

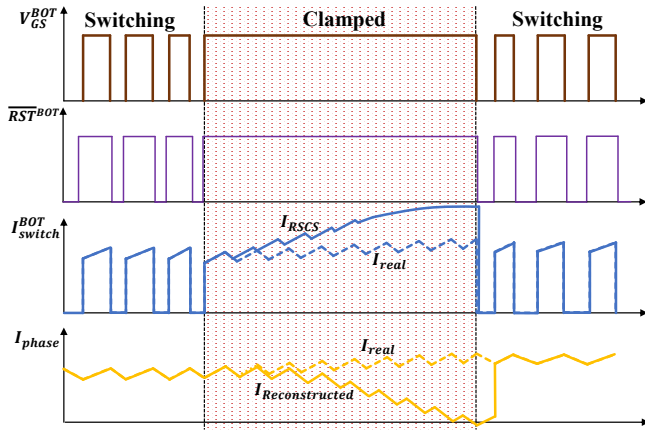


Fig. 8. Behavior of the bottom switch current sensor and phase current sensor in phase leg during DPWM

as there is a continuous PWM pulse train, active sensor reset will work and sensor output will match real currents in the system, which was experimentally verified in the previous section. When the DPWM starts, correct waveform will be observable for few switching cycles (depending on switching frequency and drifting intensity). After few switching cycles pass, on board current measurement starts to depart more and more from the real one. Since there is no reset signal coming from the FPGA, measurement will continue to drift. Controller cannot anymore rely on the measurement coming from board during this period. Experimental results for DPWM scheme case are confirmed on the Fig.9. It clearly confirms that whenever there is a clamped period in one of the phase voltages, phase current measurement coming from the corresponding gate driver will be incorrect due to RSCS drifting related problem previously described. The line frequency is

changed to 100 Hz in this case for better observation of sensor performance in the clamped period of DPWM, while the switching frequency remained the same as in continuous PWM scheme. Chosen DPWM modulation scheme is carrier-based conventional 60° DPWM, further described in the [15], and [16]. This modulation scheme is chosen due to simplicity since it is using unchanged sinusoidal reference waveforms from continuous PWM. Fundamentals of this modulation are shown on the Figure 6 in [15]. Basically, zero sequence is added to phase voltages such that resulting waveform is DPWM signal. This zero sequence will not be observed on the line-to-line voltages based on the symmetrical and balanced three phase theory, as it can be seen on Fig.9.

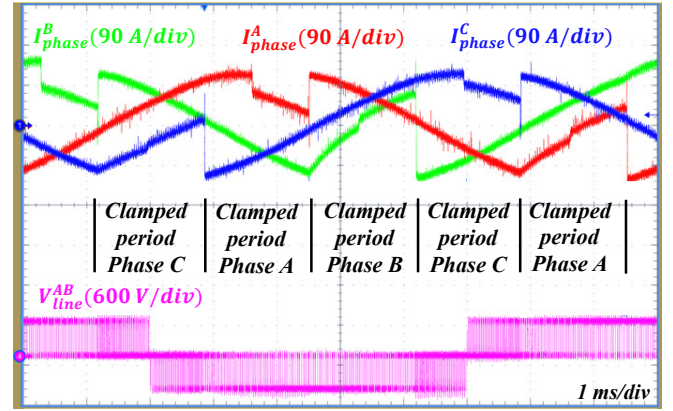


Fig. 9. Experimental results for reconstructed phase currents during DPWM scheme

In the following subsection, solution for this problem will be proposed due to a fact that DPWM schemes are often used in automotive applications to reduce losses and increase effective voltage in the system when needed.

B. Proposed software solution for DPWM schemes

Problem of inaccurate phase current during clamped period of DPWM scheme could possibly be overcome on the controller level. Three-phase motor control is intended application, meaning that the neutral point is isolated and no neutral current path exist, sum of currents in each instance will be zero (4):

$$i_a + i_b + i_c = 0 \quad (4)$$

Basically, this means that current in one of the phases can be calculated as the negative sum of the currents in the two other phases. According to DPWM fundamentals, while one phase is clamped, other two will be switching. Fact that other two phases are switching, results in valid current measurement in the switched phases, and thus the negative sum of the currents value will be correct. Based on that, whenever one phase is clamped, current in that phase can be extracted from other two phases on the controller side. This simple manipulation makes on board phase current sensor valid for both continuous and discontinuous PWM schemes. Fig.10 shows reconstruction principle idea for phase C, where green is the actual current

waveform coming from phase C gate driver. Red waveform is the one created by negative sum of the other two phase currents in the system, while blue is the real current in the system which could be obtained by combining them together during line cycle (dashed green and red on top of the blue).

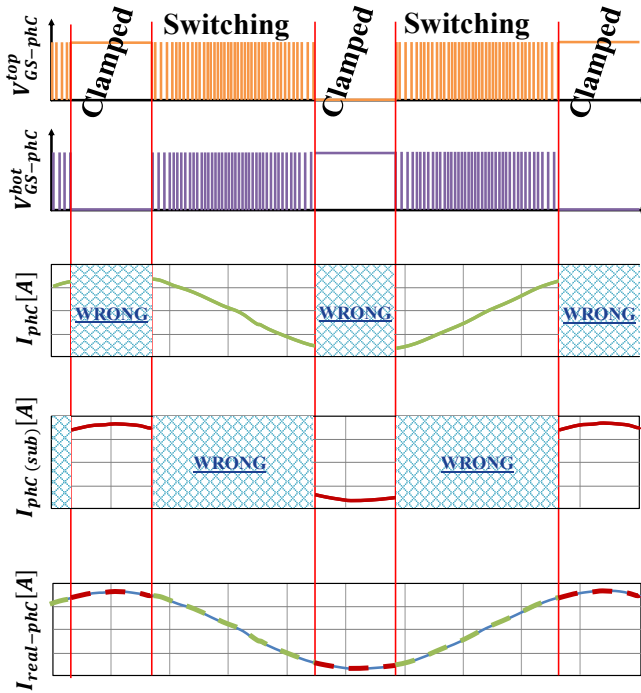


Fig. 10. Reconstruction principle during DPWM to obtain valid phase current

Simple algorithm on the controller has to be implemented in order to overcome incorrect current problem and get correct current values during whole line cycle during DPWM scheme. Implemented algorithm is proposed and validated for carrier-based two-level conventional 60° DPWM scheme. Piece of code implemented in the micro-controller interrupt routine for phase C current, right after controller reads from ADC terminals is shown on Fig.11.

Currents in the system (adc_c, adc_b, adc_a,) are constantly sampled. Based on the simple DPWM duty cycle reference (dc_zsi), it can be decided which current for corresponding phase is to be used. If duty cycle reference is clamped to either 0 or 1 (maximum value of register), reconstructed current (negative sum of other two phases) value will be used. If duty cycle reference is not clamped, current coming from corresponding GD board is correct and can be used for closed loop current control. One switching cycle delay is inserted during transition periods, from clamped to switching part of DPWM and vice versa, in order for the RSCS to reset and catch up with correct values. These delays are completely justified since system can rely on the currents coming from the phase for a few switching cycles at 30 kHz when there is no reset signal. Reconstruction algorithm can easily be verified, since online register monitoring of

```
read_adc(); // read from ADC terminals
// waveform loaded are:
// adc_c, adc_b, adc_a;

phc = adc_c; // Additional code
phc_r = - adc_a - adc_b;

if(dc_zsi_old == 0 || dc_zsi_old == 1)
{
    I_c = phc_r; // when clamped, use reconstructed
}
else
{
    I_c = phc; // when switching, use on board meas.
}
dc_zsi_old = dc_zsi; // delay until RSCS reset
// dc_zsi is inserted zero sequence
```

Fig. 11. Current reconstruction algorithm for phase C on the controller level

controller is possible. Fig.12 shows register where I_a , I_b , and I_c values are shown after reconstruction algorithm is employed, while Fig.9 shows original measured waveforms sampled by controller (multiplied with sensor gain). Values shown after reconstruction algorithm is employed are correct and are sinusoidal, even though current values on the actual ADC terminals are not correct for the whole line cycle.

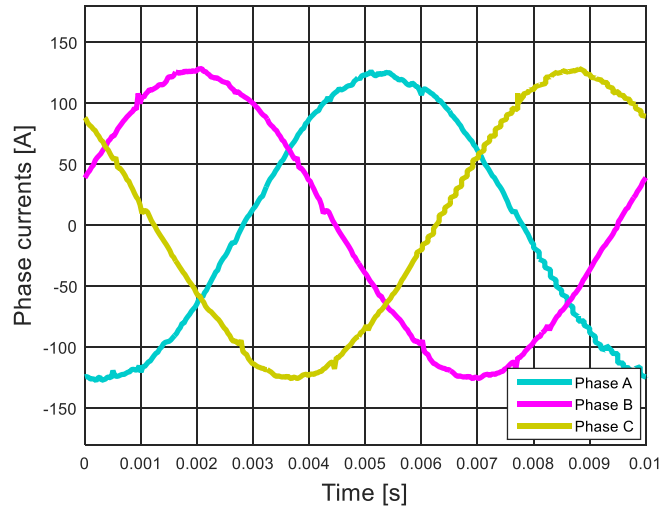


Fig. 12. Values of reconstructed phase currents stored in controller registers

Principle of current reconstruction for carrier-based two-level conventional 60° DPWM scheme is presented. For all carrier-based DPWM schemes, used principle in obtaining the valid phase current will remain the same where decision of which current information is used is made based on the DPWM duty cycle reference. However, in majority of application where DPWM schemes are required, closed loop minimum-loss space-vector modulation (min-loss SVM) is be-

ing used to further reduce switching losses by dc-bus clamping the phase-leg conducting the highest current. In this case, phase-leg clamping will be determined by the highest sensed current in the corresponding phase-leg. Due to the drifting related problems of developed phase current sensor during clamped periods of DPWM scheme, it would be difficult to determine which phase-leg and when is to be clamped, since in this case current value determines when DPWM duty cycle reference (dc_zsi) is at it's extremes. To overcome this problem in min-loss SVM, under the assumption that system is well controlled in closed loop current-wise and real currents in the system follow references, instead of measured currents being used for determining when to clamp corresponding phase-leg, reference currents should be used. With this simple alteration, developed sensor with the same algorithm shown on Fig.11 is now valid for all DPWM schemes.

V. INFLUENCE OF THE ADJACENT PHASES ON ROGOWSKI COILS

Proximity magnetic field influence of Rogowski coil measurement is investigated since inverter phase-legs are placed relatively close together and DC busbar (contains HF currents) lays on top of all of them. The Rogowski coil sensor measures the current encircled by it. However, there is a possibility of induced voltage from variable magnetic field created by the current from other 2 adjacent phases. The magnetic field created by currents in the other two phases or busbar becomes disturbance magnetic field. This disturbance magnetic field passes through coil section of the Rogowski coil together with magnetic field created by measured current and induces corresponding disturbance voltage. The disturbance voltage is superimposed on intended measurement signals, which could produce error to the measurement result if the influence is significant. Therefore, this magnetic influence has to be investigated.

Despite simple structure of Rogowski coil, in utilizing stage, it needs some special considerations to mitigate influence of disturbance fields. One step in diminishing influence of stray fields is already been done in a way that maximum turn number physically achieved based on normal PCB manufacturing techniques is realized to increase mutual inductance and intensify the output of the coil [6]. Second step was putting return conductor through inside of the the main windings. If this return was not incorporated, the Rogowski coil sensor would essentially become a one turn loop around the conductor and would be sensitive to any magnetic field that was perpendicular to the plane of the sensor [17].

Circuit used to investigate possible influence is shown on the Fig.13. Used modulation was simple sinusoidal open loop PWM modulation for full-bridge. Modulation frequency is set to be $f_m = 400\text{ Hz}$ with carrier frequency (PWM frequency) set to be $f_{sw} = 35\text{ kHz}$. In this case middle gate driver is disconnected from power supply as well as from the busbar. However, this disconnected gate driver with Rogowski coils is left mounted on the SiC MOSFET module on his location

bellow the busbar in order for us to see is there any magnetic influence coming from adjacent phases and busbar itself.

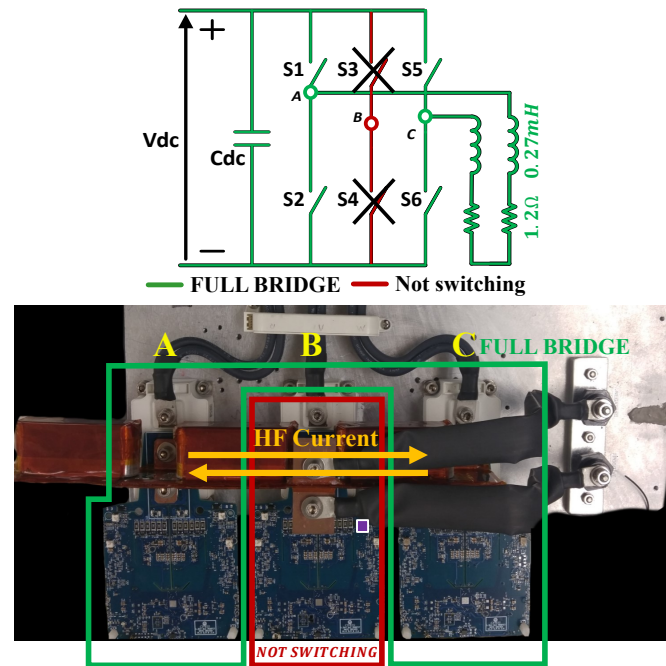


Fig. 13. Schematic and hardware for magnetic influence investigation

Output of one of the inactive Rogowski coils in the middle phase leg is indicated on Fig.13 with purple square. Ideally, this output should be clamped at 0 V if there is no magnetic influence on corresponding Rogowski coil. However, due to proximity to actually switches, low voltage probe used to measure output might pick up large amount of radiated noise. After performed test and recorded results, it is not known whether results present purely magnetic coupled noise, or this is radiated noise picked up by probe. In that sense more experiments are conducted. Probe itself is left lying next to the busbar with connected tip to the ground of the probe via very short wire. In this manner, it will be established is most of the noise picked up by the probe, or is the magnetic influence strong and observed on switching frequency and their multiples. Fig.14 shows spectral analysis results. Blue

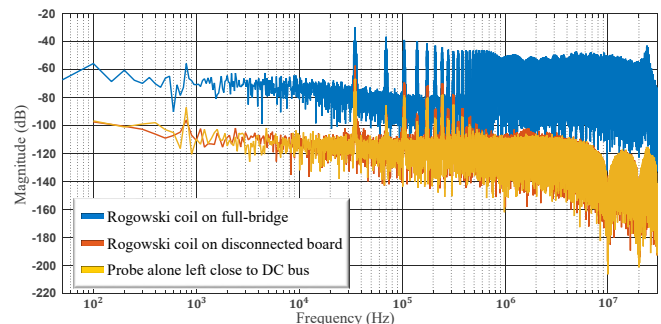


Fig. 14. Spectral analysis results for investigation of magnetic influence

waveform is output of one of the Rogowski coils which is in normal operation on one of the switched gate drivers and enabled current sensing. This waveform was recorded separately from mentioned two cases in order to be able to compare how much of magnetic coupling is actually located on the Rogowski coil on the non-switching gate driver. Orange waveform represents output of the Rogowski coil located on the the gate driver that is disconnected from the setup. Yellow waveform presents results of the probe alone sitting close to the DC bus at the same spot as in previous case with shorted probe tip to the ground of the probe in order to determine how much radiated noise is picked up by the probe itself. From Fig.14 can be seen that orange waveform is significantly smaller (roughly 40dB) than the blue waveform. However, even with this being 40db lower than employed Rogowski coil, this presents significant influence. However, from next case (yellow waveform) with probe alone placed at the same spot, it can be seen that result is almost the same as the orange waveform. There is very small difference in between these two waveforms. This means that most of the coupling effect measured in the previous case was picked up by the probe due to radiated noise and did not have to do with the actual output of the Rogowski coil and adjacent magnetic field influence. This means that magnetic coupling between adjacent legs is very small, almost negligible.

VI. CONCLUSIONS

This paper presented phase current reconstruction principle on the gate driver level using Rogowski coil switch-current sensors in the half-bridge SiC MOSFET module utilized in the voltage source inverter. With this approach, valid current information can be obtained for both continuous and discontinuous PWM schemes, with accuracy error smaller than 3 A at rated current, linearity error under 2.5 %, and delay under 1.6 μ s. For the continuous PWM, phase current information coming from the gate driver is correct and can be used directly for control purposes, while for discontinuous PWM, due to periods of inaccuracy of the phase current, simple signal conditioning algorithm has to be implemented on the main controller side, in order to obtain-reconstruct the missing part of the phase current. This opens possibility to eliminate bulky Hall-effect sensors from system and increase power density, as well as reliability due to existence of the high bandwidth current information that can be used for short-circuit protection [4]. The Rogowski coil switch-current sensor technique as well as phase current reconstruction technique could be equally applied to other technologies such as Si IGBT. Furthermore, influence of the adjacent magnetic fields is investigated and it is proven that magnetic coupling between adjacent legs is almost negligible.

ACKNOWLEDGEMENT

This material is based upon work supported by General Motors and the U.S. Department of Energy, Vehicle Technologies Office (VTO) under Award Number DE-EE-0007285, Highly

Integrated Wide Bandgap Power Module for Next Generation Plug-in Vehicles.

REFERENCES

- [1] J. Milln, P. Godignon, X. Perpi, A. Prez-Toms, and J. Rebollo, "A survey of wide bandgap power semiconductor devices," *IEEE Transactions on Power Electronics*, vol. 29, no. 5, pp. 2155–2163, May 2014.
- [2] C. M. DiMarino, R. Burgos, and B. Dushan, "High-temperature silicon carbide: characterization of state-of-the-art silicon carbide power transistors," *IEEE Industrial Electronics Magazine*, vol. 9, no. 3, pp. 19–30, Sept 2015.
- [3] J. Wang, Z. Shen, R. Burgos, and D. Boroyevich, "Integrated switch current sensor for shortcircuit protection and current control of 1.7-kv sic mosfet modules," in *2016 IEEE Energy Conversion Congress and Exposition (ECCE)*, Sept 2016, pp. 1–7.
- [4] S. Moevic, J. Wang, R. Burgos, D. Boroyevich, C. Stancu, M. Jaksic, and B. Peaslee, "Comparison between desaturation sensing and rogowski coil current sensing for shortcircuit protection of 1.2 kv, 300 a sic mosfet module," in *2018 IEEE Applied Power Electronics Conference and Exposition (APEC)*, March 2018, pp. 2666–2672.
- [5] J. Wang, Z. Shen, C. DiMarino, R. Burgos, and D. Boroyevich, "Gate driver design for 1.7kv sic mosfet module with rogowski current sensor for shortcircuit protection," in *2016 IEEE Applied Power Electronics Conference and Exposition (APEC)*, March 2016, pp. 516–523.
- [6] J. Wang, Z. Shen, R. Burgos, and D. Boroyevich, "Design of a high-bandwidth rogowski current sensor for gate-drive shortcircuit protection of 1.7 kv sic mosfet power modules," in *2015 IEEE 3rd Workshop on Wide Bandgap Power Devices and Applications (WiPDA)*, Nov 2015, pp. 104–107.
- [7] S. Ziegler, R. C. Woodward, H. H. Iu, and L. J. Borle, "Current sensing techniques: A review," *IEEE Sensors Journal*, vol. 9, no. 4, pp. 354–376, April 2009.
- [8] Z. Zhang, D. Leggate, and T. Matsuo, "Industrial inverter current sensing with three shunt resistors: Limitations and solutions," *IEEE Transactions on Power Electronics*, vol. 32, no. 6, pp. 4577–4586, June 2017.
- [9] C. Xiao, L. Zhao, T. Asada, W. G. Odendaal, and J. D. van Wyk, "An overview of integratable current sensor technologies," in *38th IAS Annual Meeting on Conference Record of the Industry Applications Conference, 2003.*, vol. 2, Oct 2003, pp. 1251–1258 vol.2.
- [10] B. R. Pelly, "Current sensing circuit for pulse width modulated motor drive," September 1998, united States Patent 5,815,391. [Online]. Available: <https://patents.google.com/patent/US5815391A/en>
- [11] S. Kim, J. Ha, and S. Sul, "Single shunt current sensing technique in three-level pwm inverter," in *8th International Conference on Power Electronics - ECCE Asia*, May 2011, pp. 1445–1451.
- [12] F. Blaabjerg and J. K. Pedersen, "A new low-cost, fully fault-protected pwm-vsi inverter with true phase-current information," *IEEE Transactions on Power Electronics*, vol. 12, no. 1, pp. 187–197, Jan 1997.
- [13] S. Moevic, J. Wang, R. Burgos, D. Boroyevich, M. Jaksic, M. Teimor, and B. Peaslee, "Phase current sensor and short-circuit detection based on rogowski coils integrated on gate driver for 1.2 kv sic mosfet half-bridge module," in *2018 IEEE Energy Conversion Congress and Exposition (ECCE)*, Sept. 2018.
- [14] Y. Liu, F. Lin, Q. Zhang, and H. Zhong, "Design and construction of a rogowski coil for measuring wide pulsed current," *IEEE Sensors Journal*, vol. 11, no. 1, pp. 123–130, Jan 2011.
- [15] A. M. Hava, R. J. Kerkman, and T. A. Lipo, "Simple analytical and graphical methods for carrier-based pwm-vsi drives," *IEEE Transactions on Power Electronics*, vol. 14, no. 1, pp. 49–61, Jan 1999.
- [16] T. Bruckner and D. G. Holmes, "Optimal pulse-width modulation for three-level inverters," *IEEE Transactions on Power Electronics*, vol. 20, no. 1, pp. 82–89, Jan 2005.
- [17] M. H. Samimi, A. Mahari, M. A. Farahnakian, and H. Mohseni, "The rogowski coil principles and applications: A review," *IEEE Sensors Journal*, vol. 15, no. 2, pp. 651–658, Feb 2015.